

Supplementary materials

Xiaolai Li,^{1,2} Binglin Zeng,^{1,2} Shuai Ren,¹ Yuliang Wang^{*,1,3}

¹ School of Mechanical Engineering and Automation, Beihang University, Beijing 100191, P. R. China

² Physics of Fluids Group, Department of Applied Physics and J. M. Burgers Centre for Fluid Dynamics, University of Twente, P.O. Box 217, 7500 AE Enschede, The Netherlands

³ Beijing Advanced Innovation Center for Biomedical Engineering, Beihang University, 37 Xueyuan Rd., Haidian District, Beijing, China

Degassing experiments for verification of gaseous nanobubbles

Two degassing experiments were performed to verify the gaseous nature of the nanobubbles. In the first experiment, we conducted experiments using the degassed water. The DI water was degassed in a vacuum chamber for 30 mins and then deposited on a PS surface immediately. The results are shown in figure S1a(I)-(III). We can barely observe the nanobubble nucleation on the immersed surface, as shown in figure S1a(II). While the phase image of figure S1a (III) shows some small dark spots, which are supposed to be nanobubbles. However, the size of these areas is much smaller than the NBs generated with air equilibrated water.

In the second degassing experiment, we first repeated experiments of nanobubble generation in our manuscript. As shown in figure S1b(I) and (II). Again we can obtain spherical cap liked nano-objects after immersion. Subsequently, the AFM fluid cell was transferred into the vacuum chamber for 1 hour degassing. After that, we found that the nano-objects became much smaller, as depicted in figure S1b(III). The above results indicate that the ‘nanobubble’ nucleation in our experiments strongly depends on the gas saturation level in the water. This proves the objects are indeed gaseous nanobubbles, not nanodroplets.

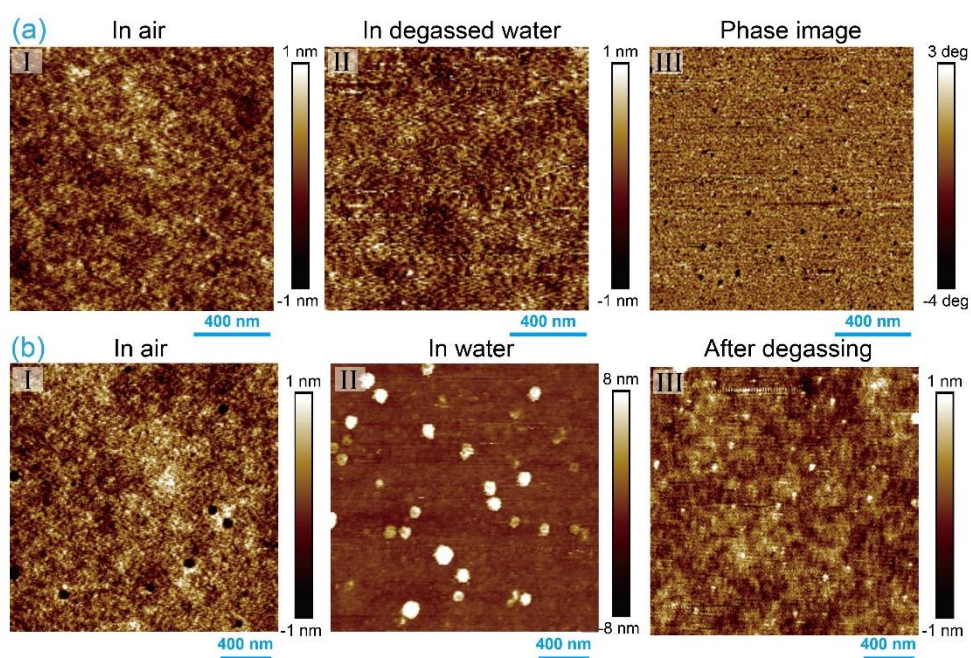


Figure S1. Degassing experimental results. (a) Nanobubble nucleation with degassed DI water. (I) AFM height image of the PS surface in air. (II) AFM height image of the PS surface immersed in degassed water. (III) AFM phase image of the water immersed surface. Very small sized nanobubbles can be seen on the surface immersed in degassed water. (b) Bubble shrinkage after degassing. AFM height image of a PS surface in air (I) and in air equilibrated water (II). (III) AFM height image after the fluid cell was transferred into the vacuum chamber. It is obvious that the nucleated nanobubbles in (II) shrunk after degassing.

Volume calculation of nanobubbles and nanodroplets

The volume of NBs and NDs before and after coalescence were measured with a home-designed image segmentation algorithm^{1, 2}. The AFM images of NBs and NDs were first segmented. This was achieved by two steps. First the NB/ND area was detected with the adaptive thresholding method, by which an initial contour was obtained. In order to achieve the optimized boundary, a contour expansion was then applied to the preliminarily detected NBs/NDs by minimizing the total energy of the contour curves¹. A NB was taken for example to show the comparison of the initial contour and the expanded contour. As displayed in figure S2, the result shows that the expanded contour can achieve a good estimation of the NB/ND boundaries. The results of the NB/ND image segmentation of Figure 1 are shown in Figure S3. With the segmented NB/ND

areas, the volume V_i of a NB/ND i can be calculated by accumulation of the volume element according to the profiles, which is given as

$$V_i = \sum_{j=1}^n h_j \Delta_s, \quad (\text{S1})$$

where Δ_s is the area element of a pixel in the segmented region, h_j is the height value of the NB/ND profile on the area element j .

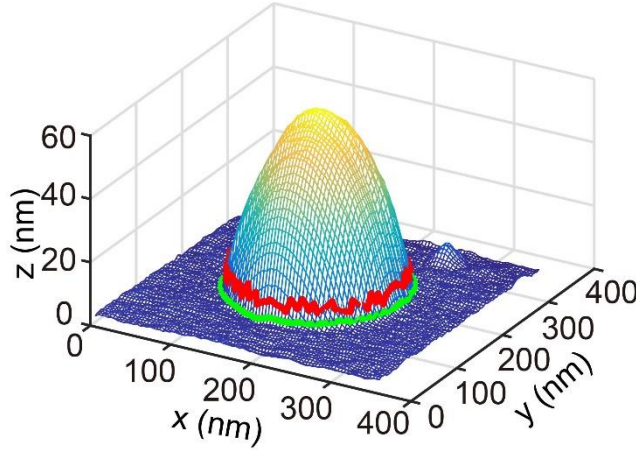


Figure S2. Mesh plot of the initial contour (in red line) and expanded contour (in green line). The result shows that the expanded contour can achieve an optimized estimation of the NB/ND boundaries.

The major source of error in the calculation of NB/ND volume comes from the boundary detection of the NB/ND images, namely the under-segmentation or over-segmentation. With the proposed method, the error in the boundary detection of NBs/NDs in this study can be minimized. Note here the distance between two neighboring points along the contour is set to be 0.3 pixel. Therefore, our segmentation can achieve a subpixel resolution. We expect the error in the boundary detection should be much smaller than one pixel. By assuming one pixel over-/under-segmentation, the obtained error of the volume calculation for bubbles in figure S2 can be estimated, as shown in figure S4. It can be seen that the error depends on the NB/ND sizes, ranging from 0.1% to 7.0%. Despite the highest error in volume calculation, the total volume increment after coalescence in table 1 in the manuscript is still pronounced for NBs.

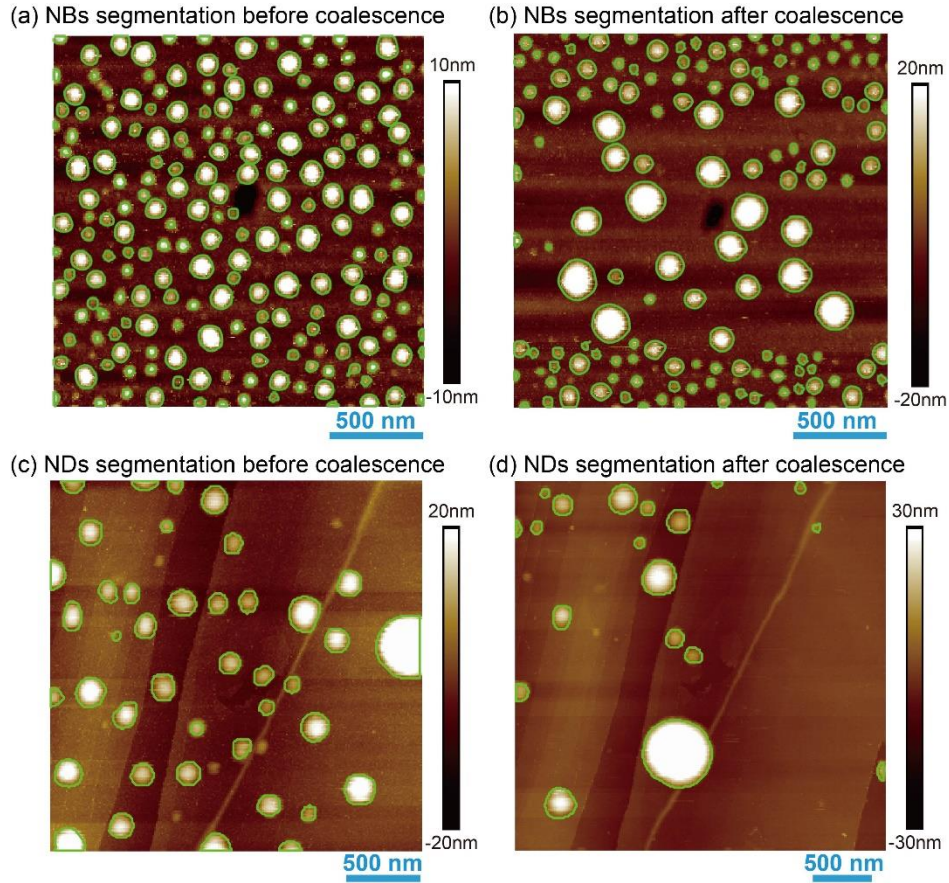


Figure S3 Segmentation results of NB height images (a-b) ND height images (c-d) shown in figure 1 in our manuscript. The green contours are the detected NB and ND boundaries. The application of contour expansion approach guarantees optimized detection of NB/ND boundaries.

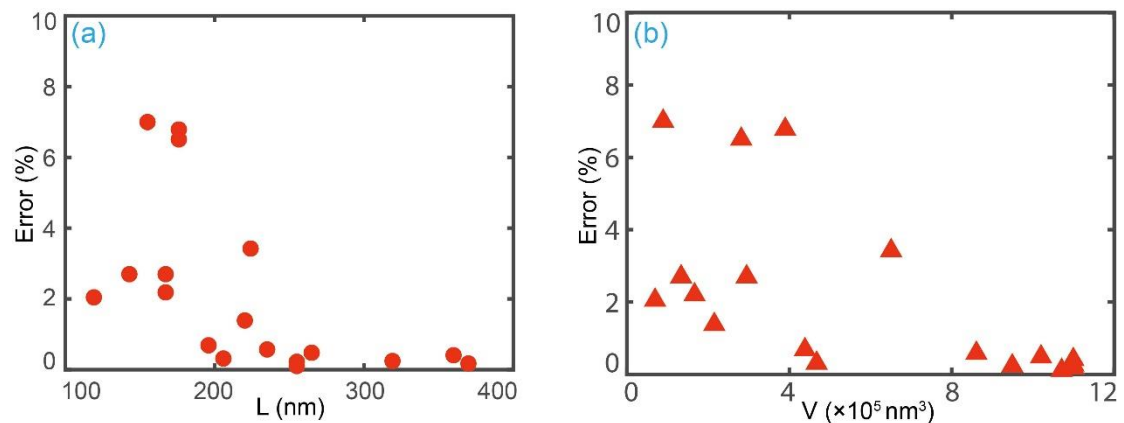


Figure S4. Error estimation for the determination of NB /ND volume. (a) The error versus the footprint L of NB/ND. (b) The error versus calculated volumes. The volume error decreases with increasing NB/ND sizes.

Repeated experiments of bubble and droplet coalescence

The NB and ND coalescence experiments were repeated to prove the volume changes. The images of NBs and NDs before and after coalescence are shown in figure S5(a-b) and (c-d), respectively. The results of the total volume in figure S5 are shown in table S1. Similar to the results of the results in table 1, the NB volume clearly increases after coalescence, while the ND volume almost remains constant. This double confirms that the NB volume increases after coalescence and verifies the gaseous nature of the ‘nanobubbles’.

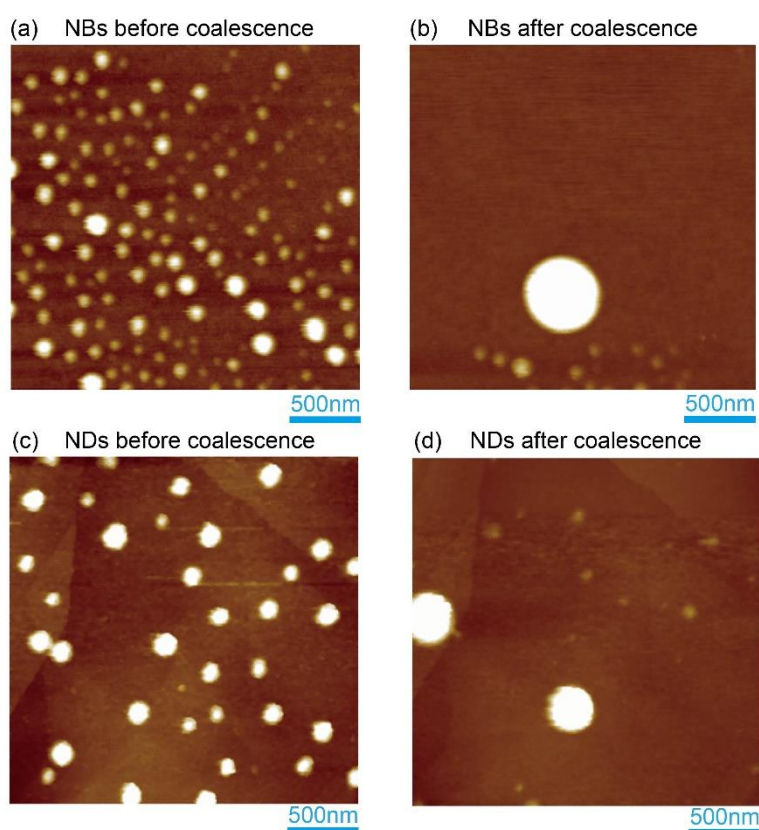


Figure S5. Repeated experiments of NB and ND coalescence

Table S1: Volume change of NBs and NDs before and after coalescence

	Before coalescence	After coalescence
$V_{nb} (\times 10^6 \text{ nm}^3)$	1.49 ± 0.10	3.09 ± 0.05
$V_{nd} (\times 10^6 \text{ nm}^3)$	2.37 ± 0.12	2.53 ± 0.07

Reference

1. Y. Wang, T. Lu, X. Li, S. Ren and S. Bi, *Beilstein Journal of Nanotechnology*, 2017, **8**, 2572-2582.
2. Y. Wang, T. Lu, X. Li and H. Wang, *Beilstein Journal of Nanotechnology*, 2018, **9**, 975-985.